IMPROVED MODELING OF THREE-PHASE TRANSFORMER ANALYSIS BASED ON MAGNETIC EQUIVALENT CIRCUIT DIAGRAMS AND TAKING INTO ACCOUNT NONLINEAR B-H CURVE

B. Kawkabani, J.-J. Simond

Swiss Federal Institute of Technology
Laboratory for Electrical Machines
EPFL-STI-ISE-LME, ELG Ecublens, CH – 1015 Lausanne, Switzerland
phone: (+4121) 693 26 80, fax: (+4121) 693 26 87
e-mail: basile.kawkabani@epfl.ch

Abstract **The present paper deals with a new approach for the study of the steady - state and transient behaviour of three-phase transformers. This approach based on magnetic equivalent circuit diagrams, takes into account the nonlinear B-H curve as well as zero-sequence flux. The nonlinear B-H curve is represented by a polynomial representation, based on a set of measurement data. For the numerical simulations, a method considering the currents as state variables has been developed, and extended to ten vector groups. Numerical results compared with test results and with FEM calculations confirm the validity of the present approach.**

1. INTRODUCTION

Traditionally in most of power system studies, the modeling of a three-phase transformer is reduced to its short-circuit impedance. Transformers used in modern power systems such as variable speed electrical drives or electrical networks with new devices (FACTS) require improved and more precise models. The B-H curve introduced in some improved models and based on a set of measurement data, is approximated generally by several straight-line segments connecting the points of measurements. But apparently, such B-H curve obtained is not smooth at the joints of the segments, and the slopes of the straight lines, representing the permeability, are discontinuous at these joints. Moreover, in the set of differential equations considering the currents as state variables, one needs the expressions of the derivatives of the inductances versus the currents, which is impossible by using the above mentioned procedure.

For that reason in the present study, the nonlinear B-H curve (or U-I curve) is represented by a polynomial representation, based on the set of measurement data. An analytical expression of a smooth B-H curve can be defined. By using a magnetic equivalent circuit-diagram representing the three-phase transformer, all the self and mutual inductances can be expressed analytically in function of the magnetic reluctances of the cores. These inductances (and their derivatives) can be determined precisely using the predetermined polynomial representation, and adapted at each integration step in the numerical simulations. The improved model obtained for the three-phase transformer, if implemented in a numerical software package, permits the analysis of saturation effects in power systems, without using systematically FEM calculations.

2. POLYNOMIAL REPRESENTATION OF THE MAGNETIC CHARACTERISTIC

A set of N+ 1 discrete measurement data I_n and ψ_n or H_n-B_n of a three-phase transformer (n=0,1,2,3,…N) is given.

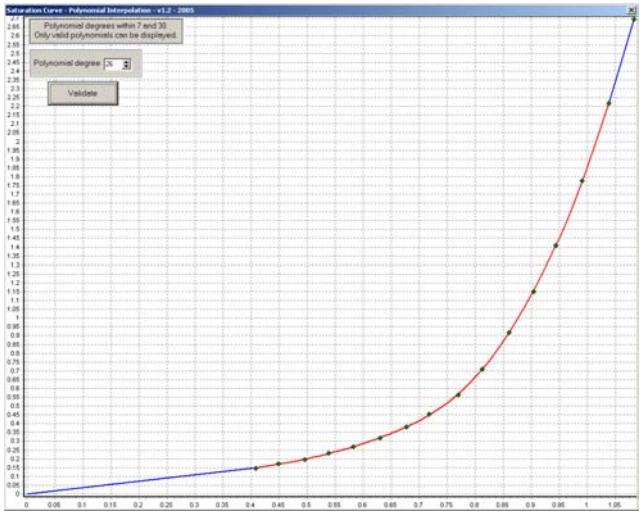

Fig. 1: Set of measured data $I-\Psi$

Three parts are considered for this polynomial representation:

- A straight-line corresponding to the linear part of this characteristic;
- A polynomial determined by a program of interpolation based on the method of least squares and fitting the measured curve;
- A straight-line corresponding to the saturated part of this curve.

The advantage of this polynomial representation comparing to Fourier series representation [1,2] is a very important gain (a factor > 5) in calculation time.

3. NUMERICAL APPROACH

Some numerical software package like SIMSEN [3] use essentially the currents as state variables. For this purpose, the present method has been developed. This one considers the following set of 9 differential equations for the vector group Yy0, for example:

$$[A]\cdot\frac{d[X]}{dt}=[B] \qquad (1)$$

with :

$$[X]^T=[iA \quad iB \quad iC \quad ia \quad ib \quad ic \quad \psi hA \quad \psi hB \quad \psi hC]$$

$$[B]=\begin{bmatrix} u_{ABC}-R_{ABC}\cdot i_{ABC} \\ u_{abc}-R_{abc}\cdot i_{abc} \\ u_{ABC}-R_{ABC}\cdot i_{ABC} \end{bmatrix} \qquad (2)$$

R_{ABC}: resistances of the primary windings
R_{abc}: resistances of the secondary windings

In this case in order to take into account saturation effects, one needs 3 supplementary state variables $\psi_{hA},\psi_{hB},\psi_{hC}$ and for the matrix [A] the expressions of all the inductances and especially all their derivatives versus the currents (dL/di). These expressions may be determined analytically by using the polynomial representation mentioned before and adapted at each integration step. The leakage inductances of the primary and secondary windings as well as the zero-sequence inductances are considered as constants.

The self and mutual inductances are expressed in function of the magnetic reluctances R_{1T}, R_{2T}, R_{3T} of the equivalent magnetic circuit-diagrams, with N_1, N_2 the turns of the primary respectively secondary windings. For example, the magnetizing inductance of the primary winding A respectively the mutual inductances L_{AB}, L_{Ab}, L_{bc} between different primary and secondary windings are given by:

$$L_{h1A}=\frac{N_1^2}{R_{1T}+\frac{R_{2T}\cdot R_{3T}}{R_{2T}+R_{3T}}}=\frac{N_1^2\cdot(R_{2T}+R_{3T})}{R_{1T}\cdot R_{2T}+R_{1T}\cdot R_{3T}+R_{2T}\cdot R_{3T}} \qquad (3)$$

$$L_{AB}=\frac{-N_1^2\cdot R_{3T}}{R_{1T}\cdot R_{2T}+R_{1T}\cdot R_{3T}+R_{2T}\cdot R_{3T}}=L_{BA} \qquad (4)$$

$$L_{Ab}=\frac{-N_1\cdot N_2\cdot R_{3T}}{R_{1T}\cdot R_{2T}+R_{1T}\cdot R_{3T}+R_{2T}\cdot R_{3T}} \qquad (5)$$

$$L_{bc}=\frac{-N_2^2\cdot R_{1T}}{R_{1T}\cdot R_{2T}+R_{1T}\cdot R_{3T}+R_{2T}\cdot R_{3T}}=L_{cb} \qquad (6)$$

Similar expressions (21 in this case) are determined for all the inductances [4]. The determination of the magnetic flux at each integration step permits to evaluate and adapt, by the B-H curve, the different magnetic reluctances as well as different inductances. An example of the determination of equations 1 and 7 is given in Appendix. Depending on the vector group studied, the number of differential equations may vary, and is equal to 11 for the vector groups Dd0 or Dd6 [4].

4. FEM CALCULATIONS

Based on the detailed knowledge of the geometry and the physical properties of different materials, 2D FEM field calculations are performed for symmetrical and unsymmetrical loads in magnetodynamics and transient behaviour.

5. MEASUREMENTS - COMPARISON OF RESULTS

Tests have been performed on two transformers:

- A small transformer of 3 kVA, 380V/232V, 50 Hz, ucc=3.26%
- A large transformer of distribution of 1 MVA, Dyn11, 18300 V/420 V, 50 Hz, ucc = 4.94 %

A. Case of no-load for a transformer Yy0 of 3 kVA, 380 V/232V, 50Hz, ucc=3.26%.

Fig. 2 shows the computed primary currents given by the numerical method and relative to a small transformer of 3 kVA in the case of no-load at rated voltage 380 V.

Fig. 3 to 5 show respectively the measured respectively computed primary currents iA, iB and iC relative to this case.

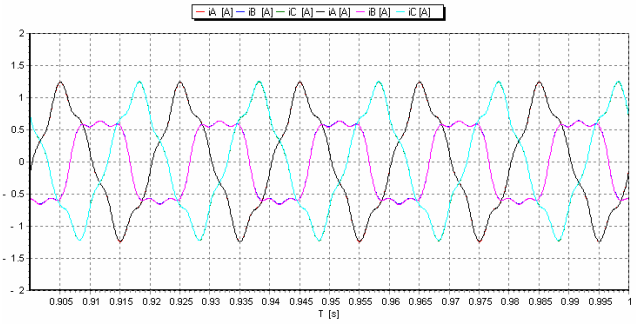

Fig. 2. Computed primary currents given by the numerical method in the case of no-load.

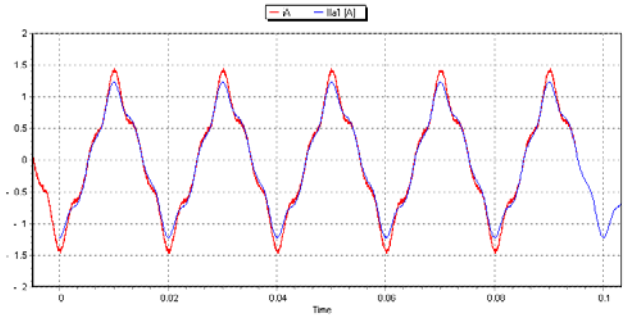

Fig. 3. Computed and measured primary currents iA in the case of no-load.

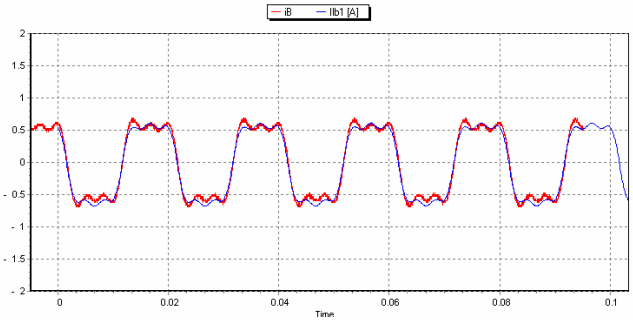

Fig. 4. Computed and measured primary currents iB in the case of no-load.

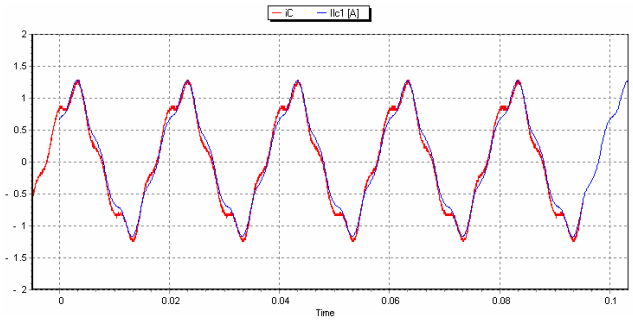

Fig. 5. Computed and measured primary currents iC in the case of no-load.

Table 1 shows results coming from different approaches in the case of no-load for a transformer Yy0, without connecting the neutrals in the primary and secondary sides.

TABLE I
COMPARISON OF RESULTS
CASE OF NO-LOAD FOR A TRANSFORMER YY0.

	Test results	Numerical approach	FEM approach
	[A]	[A]	[A]
I_A	0.803	0.745	0.75
I_B	0.52	0.515	0.531
I_C	0.76	0.744	0.749

B. Case of no-load for a transformer Dy5 of 3 kVA, U= 230V.

Fig. 6 to 8 show the measured respectively computed line primary currents relative to a coupling Dy5 in the case of no-load, under a voltage of 1.045 p.u.

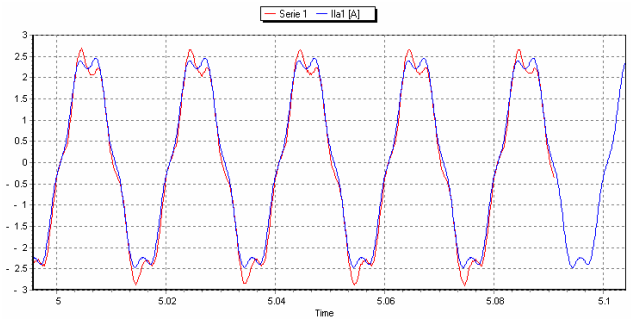

Fig. 6. Computed and measured primary currents ilA in the case of no-load.

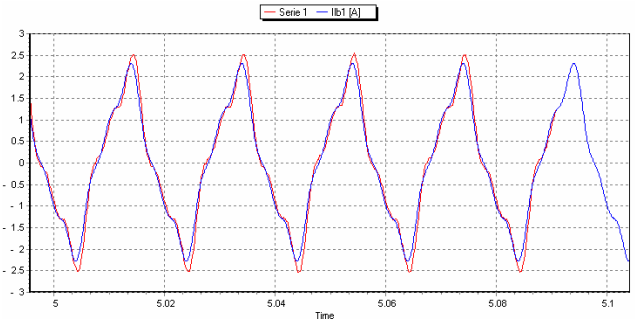

Fig. 7. Computed and measured primary currents ilB in the case of no-load.

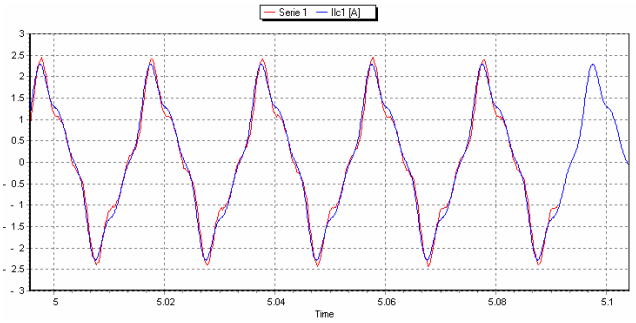

Fig. 8. Computed and measured primary currents ilC in the case of no-load.

C Case of an unsymmetrical load in the secondary of a transformer Yy0 of 3 kVA, U=U_N=380 V

Table 2 shows results coming from different approaches in the case of an unsymmetrical load connected to the secondary of the transformer (Ra = 40.5 Ω ; Rb = 14.6 Ω ; Rc = 39.15 Ω ; 63.95 % of unsymmetry) under rated voltage U_N= 380 V, with the neutral connected only in the secondary side. A measured zero-sequence reactance is taken into account in the secondary side L_{os}=1.9 mH. A very good agreement between results coming from different approaches can be noticed (relative error less than 8 % between different approaches).

TABLE II
COMPARISON OF RESULTS

	Test results	Numerical approach	FEM approach
	[A]	[A]	[A]
I_A	2.62	2.50	2.55
I_B	4.46	4.33	4.30
I_C	3.41	3.2	3.15
I_a	3.2	3.2	3.22
I_b	9.17	8.89	8.82
I_c	3.42	3.45	3.39

D. Case of a no-load switching of a transformer Dd0 of 3 kVA, U= 221.4V.

The studied transformer T1 is supplied by a source voltage VS and an autotransformer T2 (Fig. 9). Fig. 10 to 12 show the measured respectively computed line primary currents

relative to a coupling Dd0 in the case of a no-load switching, under a voltage of 1.006 p.u. Fig. 13 shows the measured respectively computed line primary voltages Uab1 in this case.

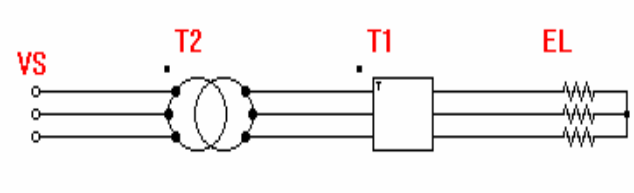

Fig. 9. Studied system

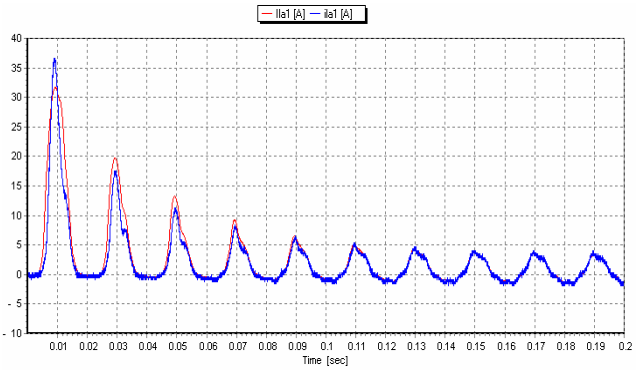

Fig. 10. Computed and measured primary currents ila1 in the case of a no-load switching.

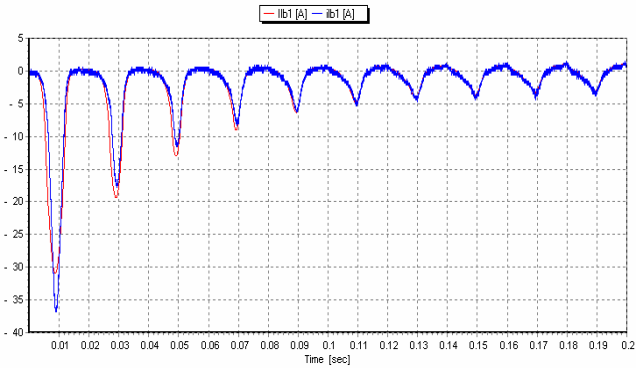

Fig. 11. Computed and measured primary currents ilb1 in the case of a no-load switching.

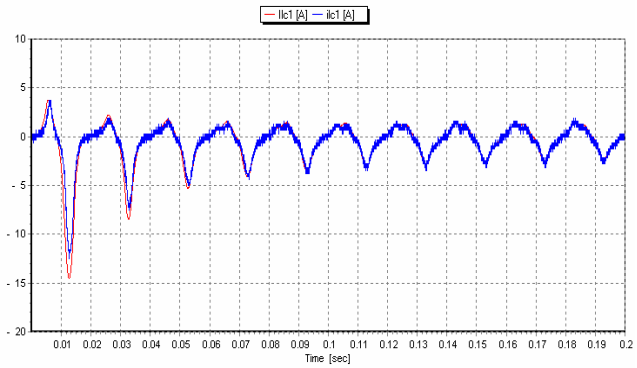

Fig. 12. Computed and measured primary currents ilc1 in the case of a no-load switching.

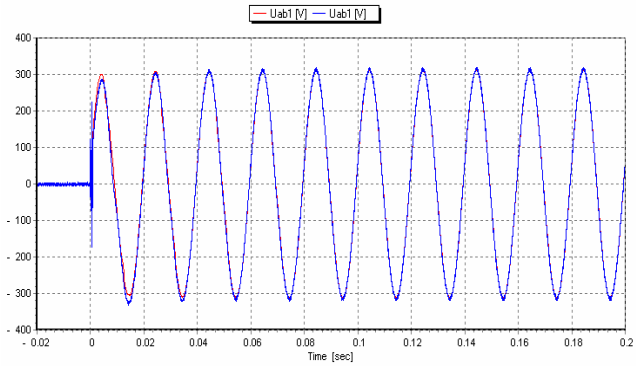

Fig. 13. Computed and measured line primary voltages Uab1 in the case of a no-load switching.

E. Case of a no-load switching of a large transformer of distribution Dyn11 of 1 MVA, 18300/420 V.

Fig. 14 to 16 show the measured respectively computed line primary currents in the case of a no-load switching, under rated voltage of 1 p.u. Fig. 17 to 19 show the measured respectively computed line secondary voltages Uab2, Ubc2, Uca2 in this case.

One can notice very good agreement between results coming from numerical and test results.

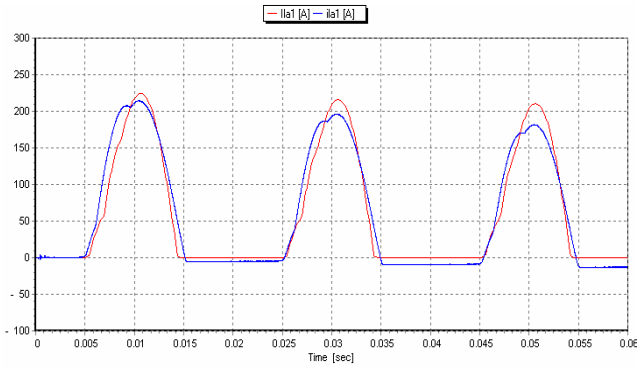

Fig. 14. Computed and measured primary currents ila1 in the case of a no-load switching.

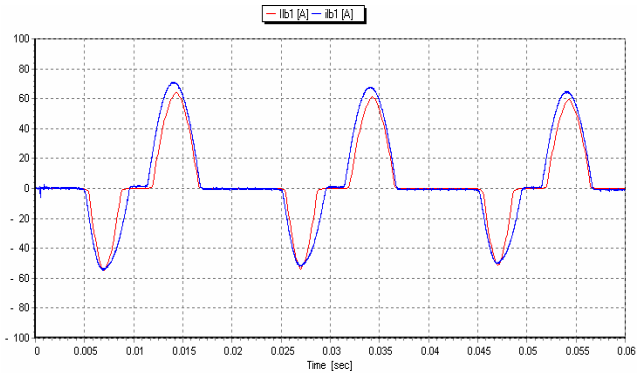

Fig. 15. Computed and measured primary currents ilb1 in the case of a no-load switching.

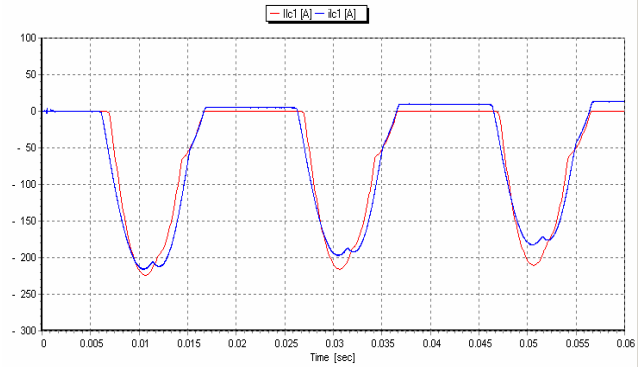

Fig. 16. Computed and measured primary currents ilc1 in the case of a no-load switching.

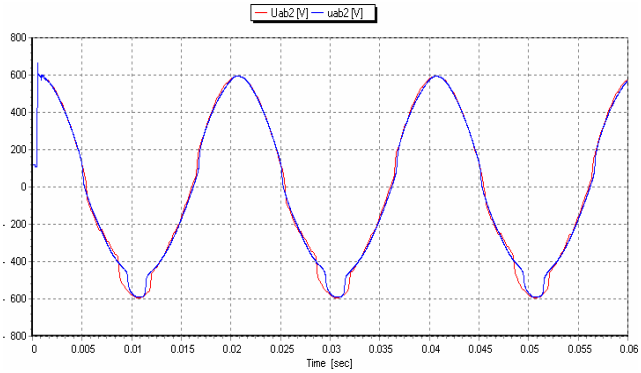

Fig. 17. Computed measured line secondary voltages Uab2 in the case of a no-load switching.

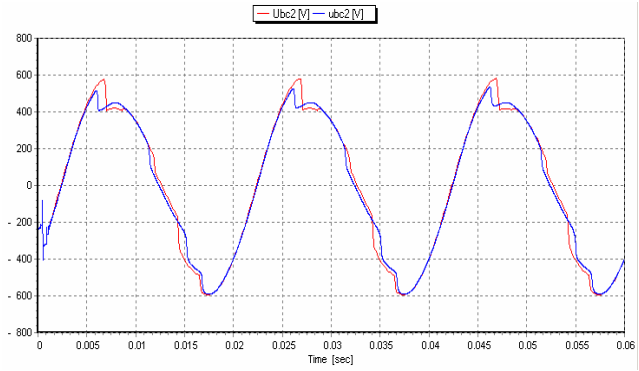

Fig. 18. Computed and measured line secondary voltages Ubc2 in the case of a no-load switching.

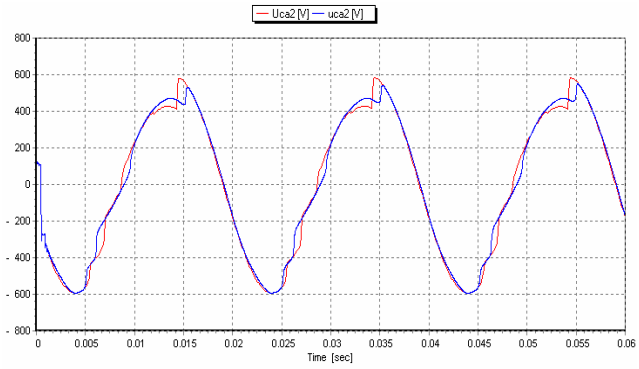

Fig. 19. Computed and measured line secondary voltages Uca2 in the case of a no-load switching.

The present method has been applied and extended [4] to the following ten vector groups (Yy0, Yy6, Dd0, Dd6, Dy5, Dy11, Yd5, Yd11, Yd1, Yd7).

6. CONCLUSIONS

In the present paper, a new approach for the three-phase transformer analysis is described. This one based on equivalent magnetic circuit-diagrams takes into account the nonlinear B-H curve and zero-sequence flux. The B-H curve is represented by a polynomial representation which gives a smooth B-H curve, and permits the analytical determination of all the inductances and their derivatives versus the currents. Numerical results compared with test results and with FEM calculations confirm the validity of the present approach, and show a very good agreement between results coming from different approaches.

APPENDIX

Voltage equations (vector group Yy0)

Equation 1 is given by :

$$u_A = R_A \cdot i_A + \frac{d\psi_A}{dt} = R_A \cdot i_A + (L_{\sigma A} + L_{h1A}) \cdot \frac{di_A}{dt} + L_{AB} \cdot \frac{d}{dt} i_B + L_{AC} \cdot \frac{d}{dt} i_C + L_{Aa} \cdot \frac{d}{dt} i_a + L_{Ab} \cdot \frac{d}{dt} i_b + L_{Ac} \cdot \frac{d}{dt} i_c + \frac{d\psi_{hA}}{dt}\{Val1\} + \frac{d\psi_{hB}}{dt}\{Val2\} + \frac{d\psi_{hC}}{dt}\{Val3\} \quad (A.1)$$

with :

$$Val1 = \frac{dR_{1T}}{d\psi_{hA}} (i_A \cdot \frac{\partial L_{h1A}}{\partial R_{1T}} + i_B \cdot \frac{\partial L_{AB}}{\partial R_{1T}} + i_C \cdot \frac{\partial L_{AC}}{\partial R_{1T}} + i_a \cdot \frac{\partial L_{Aa}}{\partial R_{1T}} + i_b \cdot \frac{\partial L_{Ab}}{\partial R_{1T}} + i_c \cdot \frac{\partial L_{Ac}}{\partial R_{1T}}) \quad (A.2)$$

and

$$\frac{\partial L_{h1A}}{\partial R_{1T}} = \frac{-N_1^2 \cdot (R_{2T} + R_{3T})^2}{(R_{1T} \cdot R_{2T} + R_{1T} \cdot R_{3T} + R_{2T} \cdot R_{3T})^2} \quad (A.3)$$

$$\frac{\partial L_{AB}}{\partial R_{1T}} = \frac{N_1^2 \cdot R_{3T} \cdot (R_{2T} + R_{3T})}{(R_{1T} \cdot R_{2T} + R_{1T} \cdot R_{3T} + R_{2T} \cdot R_{3T})^2} \quad (A.4)$$

$$\frac{\partial L_{AC}}{\partial R_{1T}} = \frac{N_1^2 \cdot R_{2T} \cdot (R_{2T} + R_{3T})}{(R_{1T} \cdot R_{2T} + R_{1T} \cdot R_{3T} + R_{2T} \cdot R_{3T})^2} \quad (A.5)$$

$$\frac{\partial L_{Aa}}{\partial R_{1T}} = \frac{-N_1 \cdot N_2 \cdot (R_{2T} + R_{3T})^2}{(R_{1T} \cdot R_{2T} + R_{1T} \cdot R_{3T} + R_{2T} \cdot R_{3T})^2} \quad (A.6)$$

$$\frac{\partial L_{Ab}}{\partial R_{1T}} = \frac{N_1 \cdot N_2 \cdot R_{3T} \cdot (R_{2T} + R_{3T})}{(R_{1T} \cdot R_{2T} + R_{1T} \cdot R_{3T} + R_{2T} \cdot R_{3T})^2} \quad (A.7)$$

$$\frac{\partial L_{Ac}}{\partial R_{1T}} = \frac{N_1 \cdot N_2 \cdot R_{2T} \cdot (R_{2T} + R_{3T})}{(R_{1T} \cdot R_{2T} + R_{1T} \cdot R_{3T} + R_{2T} \cdot R_{3T})^2} \qquad \text{(A.8)}$$

Similar expressions may be written for Val2 and Val3, as well as for the derivatives of the inductances versus R_{2T} and R_{3T}.

Equation 7 may be written as:

$$u_A = R_A \cdot i_A + L_{\sigma A} \cdot \frac{di_A}{dt} + \frac{d\psi_{hA}}{dt} \qquad \text{(A.8)}$$

ACKNOWLEDGMENT

We are grateful to Mr Sidney Mattatia and Mr Bernard Bugnon from the management of the Electricity Company in Geneva - SIG for allowing different tests in their laboratories on a large transformer of distribution of 1 MVA. We are also grateful to Mr Christian Fleury and his team from SIG, and to our colleague Mr Roland Wetter to their valuable contributions on these tests. Many thanks to Mr Harry Zueger from ABB Sécheron SA for providing us different data concerning this large transformer.

REFERENCES

[1] Guanghao L., Xiao-Bang Xu, "Improved Modeling of the Nonlinear B-H Curve and Its application in Power Cable Analysis", *IEEE Transactions on magnetics*, vol. 38,No 4, pp. 1759-1763, July 2002.

[2] Kawkabani B., Simond J.-J., "Improved modelling of three-phase transformer analysis based on nonlinear B-H curve and taking into account zero-sequence flux", XVI International Conference on Electrical Machines ICEM 2004, Cracow, Poland, September 2004.

[3] Simond J.-J.,Sapin A.,Kawkabani B.,Schafer D., Tu Xuan M., Willy B., "Optimized Design of Variable-Speed Drives and Electrical Networks", *7th European Conference on Power Electronics and Applications EPE'97*, Trondheim, Norway, September 1997.

[4] Kawkabani B. "Modélisation d'un transformateur triphasé à 3 colonnes avec prise en compte de la saturation et des flux homopolaires. Etude de 10 couplages'', *Internal report EPFL No 05/101,* Lausanne, Switzerland, February 2005.

[5] FLUX2D, version 7.60/6b, CEDRAT.